Clim. Past Discuss., 9, 3993–4034, 2013
www.clim-past-discuss.net/9/3993/2013/
doi:10.5194/cpd-9-3993-2013

Climate of the Past Discussions
Open Access

Past freeze and thaw cycling in the margin of the El'gygytgyn Crater deduced from a 141 m long permafrost record

G. Schwamborn[1], **H. Meyer**[1], **L. Schirrmeister**[1], **and G. Fedorov**[2]

[1]Alfred Wegener Institute for Polar and Marine Research, Telegrafenberg A43, 14473 Potsdam, Germany
[2]Arctic and Antarctic Research Institute, Bering Street 38, 199397 St. Petersburg, Russia

Received: 14 June 2013 – Accepted: 2 July 2013 – Published: 16 July 2013

Correspondence to: G. Schwamborn (georg.schwamborn@awi.de)

Published by Copernicus Publications on behalf of the European Geosciences Union.

Abstract

Past permafrost thaw and freeze has destabilised the basin slopes of Lake El'gygytgyn in the northeastern Eurasian Arctic. This has probably promoted the release of mass movements from the lake edge to the deeper basin as known from frequently occurring turbidite layers in the lake sediment column. The continuous sediment record from the Arctic spans the last 3.6 Ma and for much of this time permafrost dynamics and lake level changes likely have played a crucial role for sediment delivery to the lake. Changes in the ground ice hydrochemical composition (pH, $\delta^{18}O$, δD, electrical conductivity, Na^+, Mg^{2+}, Ca^{2+}, K^+, HCO_3^-, Cl^-, SO_4^-) of a 141 m long permafrost record from the western crater plain are examined to reconstruct repeated freeze and thaw cycles at the lake edge. Stable water isotope and major ion records of ground ice in the permafrost reflect both a synsedimentary palaeo-precipitation signal preserved in the near-surface permafrost (0.0 m to 9.1 m core depth) and a postdepositional record of talik thawing and refreezing in deeper layers of the core (9.1 to 141.0 m core depth). The lake marginal permafrost dynamics were controlled by lake level changes that episodically flooded the surfaces and induced thaw in the underlying frozen ground. At least three cycles of freeze and thaw during marine isotope stage (MIS) 7, possibly MIS 5, and the Allerød (AD) are identified and the hydrochemical data point to a vertical and horizontal talik refreezing through time.

1 Introduction

The level of Lake El'gygytgyn, which developed in the 3.6 million years old impact crater in the Eurasian Arctic (Layer, 2000), has changed several times, at least during the Late Quaternary (Glushkova and Smirnov, 2007; Schwamborn et al., 2008; Juschus et al., 2011). Recently the basin fill was cored and a unique 312 m long Plio-Pleistocene lake sediment record (core 5011-1) was retrieved, which is being explored for palaeoclimatic and palaeoenvironmental reconstruction (Melles et al., 2012; Brigham-Grette et al.,

CPD
9, 3993–4034, 2013

2013). Additionally, a 141 m long permafrost core (core 5011-3) was taken from the western crater margin for studying catchment-to-lake interaction in the past (Fig. 1). Interpretation of the permafrost core sediments suggests that there is a close linkage between alluvial fan growth on the slopes and the sediment delivery to the lake (Schwamborn et al., 2012). The prograding sediment transport in alluvial fan systems has probably initiated frequent sliding events into the lake basin as found in seismic lines (Niessen et al., 2007) and in lake cores (Juschus et al., 2009). Recently, 37 % of the Quaternary sediment series in lake core 5011-1 were found to consist of mass movement deposits (Sauerbrey et al., 2013). Next to prograding sediment transport permafrost thaw and freeze might be another cause of sediment release to the basin, because during periods of rising lake level the marginal permafrost thaws in the inundated areas and slope material becomes destabilised. In order to better understand the permafrost-dependent (i.e. freezing-front-dependent) sediment delivery to the basin, determining the ground ice composition and its origin helps to complete the understanding of the lake marginal depositional history. Today's catchment-to-lake ratio is only 1.6 : 1 and it is expected that the growth and shrinking of the catchment area in the course of Quaternary lake level changes potentially exerted a large influence on the amount and nature of material released into the basin.

The history of talik development (i.e. an unfrozen zone below the lake surrounded by permafrost) is likely stored in the permafrost pore water chemistry; the study of this chemistry in order to elucidate the history is the subject of the present paper. The stable isotope composition in the ground ice of core 5011-3 can give evidence on water origin (precipitation versus lake water) and isotope modification through fractionation during phase transitions (i.e. freezing). Under peculiar conditions the ground ice also may have preserved a climatic signal (see Schwamborn et al., 2006). Variations of the stable water isotope composition in natural environments have been widely used in the interpretation of past polar climatic and environmental conditions. Ground ice has been analysed to infer climate history in non-glaciated terrain (Meyer et al., 2010a, b; Opel et al., 2011) or to elucidate the origin of Antarctic permafrost (Stuiver and Yang, 1981;

CPD
9, 3993–4034, 2013

Swanger et al., 2010). Other ground ice research has been used to infer combined palaeoenvironmental and palaeoclimatic change in the terrestrial Arctic (Lacelle et al., 2004; Wetterich et al., 2011; Vasil'chuk et al., 2012) or to aid the genetic interpretation of water sources in permafrost terrain (e.g. Mackay, 1983; Leibman, 1996; Dereviagin et al., 2003; Lacelle et al., 2004, 2009).

Permafrost aggradation at any given site is accompanied by pore water freezing in situ or migrating to form ice lenses. Ion and O-H isotope fractionation are known to be affected by freezing and diffusion rates (Souchez et al., 2000; Lacelle et al., 2009; Fritz et al., 2011; Michel, 2011); therefore, the first ice to form will have heavier δ^{18}O and δD values (and a lower d excess) than the last ice. Gradients are expected to result from lateral, down- or upward permafrost growth even in homogenous material with an initial uniform groundwater quality. Following Lacelle (2011), the first ice to form will be enriched in ^{18}O by about 3 ‰ (and about 20 ‰ in D) as freezing begins, but as freezing continues, the δ^{18}O composition of the forming ice becomes progressively depleted as the δ^{18}O composition of the residual water trends toward lower values. Conversely, freezing of liquid water leads to a progressive increase in d excess even to values of > 10 ‰ above the GMWL (Fritz et al., 2011).

There have been various attempts to correlate and explain the co-isotope slopes of ice and water frozen under a variety of conditions. As noted in Mackay (1998, and references cited therein), the slopes alone have usually been difficult though to interpret in both glacial and periglacial studies. In all cases, it was recommended that stable O-H isotope measurements should be supported by the use of additional distinguishing tools as are discussed below when attempting to infer ground ice genesis (Lacelle, 2011).

Changes in the downcore light soluble salts are one additional indicator of permafrost degradation and aggradation. When permafrost aggrades in moist sediments, the chemical composition of the newly formed ground ice differs from the unfrozen pore water. Previous studies show that ice formation is linked to solute redistribution, because solutes are excluded from the crystal lattice as water freezes (e.g. Mackay

CPD
9, 3993–4034, 2013

and Lavkulich, 1974; Hallet, 1978; Mahar et al., 1983; Kadlec, 1984; Ostroumov et al., 2001). This causes differentiated solute redistribution at permafrost sites with multiple but non-equal freeze and thaw cycles of different waters. A spatially inhomogeneous concentration pattern may thus reflect a differentiated retreat and advance of the freezing front, which causes a solute redistribution in the subground and variations in the ground ice record. A prominent example is the active layer (i.e. seasonally thawed soil layer), where soil moisture is annually redistributed and the last soil layer to refreeze has the lowest δ values and the highest ion concentration (Ostroumov et al., 1998). Ground ice with low soil solute concentration points to surfaces that were subject to progressive removal of soluble material as deeper permafrost thawed (Kokelj and Burn, 2005). Especially in freezing sandy environments the solutes migrate to the unfrozen zone (Qiu et al., 1988). However, if freezing takes place rapidly enough the leaching of saline pore water can be prevented almost completely as has been observed in emerged marine sediments (O'Sullivan, 1963).

The aim of this paper is to highlight a subject that has been little studied to date, the effect of sediment freezing on the pore water hydrochemical composition and the interpretation of connected past environmental change. The assumption that the output from this research will help to advance our understanding of the long-term lake and permafrost processes that have shaped the unique Lake El'gygytgyn archive stimulated the study. This paper complements the sedimentological approach of Schwamborn et al. (2012) by focusing on the hydrochemical aspects (i.e. changes in stable water isotopes and in ion concentration) of the 5011-3 permafrost record.

2 Environmental setting

El'gygytgyn Crater is a roughly circular depression, 18 km in diameter, and partially occupied by a lake that is 12 km in diameter (Fig. 1). The hills on the crater rim rise to between 600 and 930 m a.s.l. (asl), and the lake level is 492 m a.s.l. Fifty seasonally active inlet streams drain the crater slopes and loose Quaternary deposits cover the

CPD
9, 3993–4034, 2013

crater plain surrounding the lake. The active layer is about 0.4 m deep in peaty silts and can reach 0.5–0.8 m in sand and gravels on the slopes. The site is in the continuous permafrost zone with a MAAT (mean annual air temperature) of −10 °C at 3 m above the ground (Nolan and Brigham-Grette, 2007). Air temperature extremes in 2002 ranged from −40 °C to +26 °C and precipitation comprised 70 mm of summer rainfall (June–September) and 110 mm water equivalent of snow (Nolan and Brigham-Grette, 2007). The MAGT (mean annual ground temperature) below the area of seasonal temperature cycling is −6.1 °C at 20 m depth with a total permafrost thickness between 330 and 360 m calculated from borehole temperature measurements at site 5011-3 (Mottaghy et al., 2013).

Both beneath the surface and above the shoreline of the presently 170 m deep (at maximum) bowl-shaped lake there is a series of terrace remnants, which mark ancient shoreline positions. Glushkova and Smirnov (2007) mapped two ancient shorelines based on subaerial terrace remnants, which are tentatively attributed to the "Middle Pleistocene" at 35–40 m above the present lake level (+40 m terrace) and the "Late Pleistocene" at 9–11 m above the present lake level (+10 m terrace). Schwamborn et al. (2008) dated an Allerød (AD) lake level at 3–4 m above the present lake level (+4 m terrace). In addition, Juschus et al. (2011) recognised a subaquatic terrace at 10 to 12 m below the present lake level and attributed it to the "Last Glacial Maximum (LGM)" (−10 m terrace).

The 5011-3 coring position (76°29.10′ N, 171°56.70′ E) is located in the central part of the western permafrost flat (Fig. 2). The core position lies 8 m higher than the lake level on a gently sloping surface (< 4°). To the east the closest shore bars are 350 m away, and to the west the nearest volcanic bedrock occurs 4 km upslope. The area between is covered by talus and slope material. A hummocky tundra environment characterizes the surface with a loamy to rubbly substrate. Surface drainage occurs mainly during spring snowmelt. The ground is mostly dry in summer. Creeks are intermittent and ponds do not persist. The coring site is located at the distal end of a sediment

CPD
9, 3993–4034, 2013

fan that is the most distinctive sediment body on the western-to-northern braid plain; several fans in a row cover this area (Schwamborn et al., 2012).

3 Methods

Core 5011-3 reached a depth of 141 m with 91 % core recovery. The strata were entirely frozen when recovered. On site, the core sections were initially described and photographically documented. They were kept frozen in the field and during transport to the laboratory, where the cores were cleaned, the documentation was completed, and subsamples were taken from the sediment and the ground ice for further laboratory analyses. On average, samples were taken every 0.5 m or where a sediment change occurred. Sections were 15 to 20 cm long and had a gross weight of about 2 to 3 kg. Frozen samples stored in polyethylene bags were weighed, thawed, and allowed to settle. Thawed ground ice was immediately extracted from the samples using pore water samplers (i.e. rhizones; Seeberg-Elverfeldt et al., 2005). The extracted water was analysed for pH and electrical conductivity (EC) using a WTW Multilab 540. Subsamples were taken for stable water isotope and main cation and anion analyses.

Hydrogen and oxygen isotope ratios were measured on a Finnigan MAT Delta-S mass spectrometer and are presented using δ notation representing the per mille (‰) relative difference with respect to Vienna Standard Mean Ocean Water (VSMOW). The measuring procedure is described in Meyer et al. (2000). Internal 1σ error is better than 0.1 % for δ^{18}O and 0.8 % for δD. The results are presented in δ^{18}O-δD diagrams with respect to the Global Meteoric Water Line, a correlation of surface waters and precipitation with a slope of 8 (GMWL; $\delta D = 8\,\delta^{18}O + 10$; Craig, 1961; Rozanski et al., 1993). In addition, the deuterium excess d ($d = \delta D - 8\,\delta^{18}O$; Dansgaard, 1964) gives evidence on the deviation from the GMWL and helps to elucidate the kinetic (i.e. non-equilibrium) fractionation processes. The d excess is affected by relative humidity during the formation of primary vapour masses. On a global scale d excess for precipitation averages +10 ‰; it is reduced to values near 0 ‰ and lower by non-equilibrium fractionation dur-

CPD
9, 3993–4034, 2013

ing subsequent phase changes, including evaporation or freezing of moisture when ground ice formed (Lacelle et al., 2004).

The major cation concentrations (Na^+, Mg^{2+}, Ca^{2+}, K^+) of the ground ice water samples were determined by optical emission spectrometry (Inductively Coupled Plasma – Optical Emission Spectrometer ICP-OES; Optima 3000 XL, PerkinElmer). The anions (Cl^-, SO_4^-) were assessed using ion chromatography (Dionex DX-320). HCO_3^- concentrations were measured immediately after rhizon sampling by titration with 0.01 M HCl using an automatic titrator (Metrohm 794 Basic Titrino). Ion concentrations are expressed in millimol-equivalents per litre (meq L^{-1}). A total of 286 samples were used for measurements and ion balance calculations using the following equation:

$$x = \left(\sum \text{cations} - \sum \text{anions}\right) / \left(\sum \text{cations} + \sum \text{anions}\right) \quad (1)$$

A relative uncertainty of less than 10 % (related to half of the sum of cations and anions) was accepted, since the overall EC in the record is low. The ionic balance uncertainty was > 10 % for only five samples, which are from between 4.0 and 8.0 m core depth.

The remaining sample parts were freeze-dried and then the absolute ice content was determined and is expressed as total water content equivalent in weight percentage (wt%) of the moist sample. The solid portion of the sample underwent a standard suite of sediment analyses, which is described elsewhere (Schwamborn et al., 2012). Precipitation (snow and rain) and surface water from the lake and tundra ponds were sampled between early May and late August 2003.

4 Results

4.1 Sediment strata and ground ice occurrence

The ground ice record of core 5011-3 developed in mostly matrix-supported sandy gravel to gravelly sand (Fig. 2). The sediment interpretation of core 5011-3 concluded

CPD
9, 3993–4034, 2013

that the strata belong to different portions of a prograding fan delta that enters Lake El'gygytgyn from the west (Schwamborn et al., 2012). Between 141.0 and 117.0 m core depth several thin (< 5 cm thick) sand layers intercalate with sandy gravel and are interpreted to be the bottomset facies of prodelta sediments, which were deposited in deeper water. The sandy gravel that is encountered between 117.0 and 24.3 m core depth most likely formed as a foreset facies of the debris cone in the delta front. Between 24.3 and 8.5 m core depth various thick (< 15 cm) sandy layers, especially from 24.0 to 19.0 m and 9.6 to 9.1 m core depth, are interpreted as flooding horizons from lake level highstands. The upper 9.1 m of core are interpreted to be a topset facies consisting of slope creep deposits and creek channel fill.

Overall the ground ice in 5011-3 is structure-less pore ice that mostly formed as ice cement, i.e. the intrasedimental ice filled the available pore space within the sediment layers. Occasionally the ground ice formed crusts < 1 cm thick around gravel-sized clasts, or ice inclusions, where the sediment packing was looser. Some sediment samples show ice-filled cracks suggesting that ice veins healed the ruptured sediment at a postsedimentary stage when the slope was not fully frozen. These cracks are nearly vertical in orientation, commonly 1–2 cm thick and up to 10 cm long, e.g. at 93.4 m, 70.4 m, 70.05 m, 68.4 m, 66.8 m, 64.4 m, 46.3 m, 44.5 m, 41.3 m, 40.9 m, and 19.5 m core depth. Photographic examples of the sediments and ground ice features are given in Fig. 2.

4.2 Hydrochemical zonation

Based on the hydrochemical data the core is subdivided into seven hydrochemical zones (HZs). The zones are best defined by the EC and the associated changes in ion load. The EC changes are fairly well reflected in the other measured properties and are graphically displayed in Figs. 3 and 4. $\delta^{18}O$ and δD and d excess with mean, minimum and maximum values are listed in Table 1, in addition. In the following the zones are described from the bottom to the top.

CPD
9, 3993–4034, 2013

HZ 1 (141.0–123.0 m)

Both water content and variability are low in this unit (mean: 12 wt%), the stable isotope variability is low (δ^{18}O mean: −21.8 ‰; δD mean: −167.6 ‰; *d* excess mean: 6.7 ‰), the slightly basic pH values show little variability (pH mean: 7.3) (Fig. 3), and the EC values (EC mean: 51 µS cm^{-1}) and the corresponding ion load (1.14 meq L^{-1}) are low. Overall the water is enriched in $Na^+ + K^+$ cations over Ca^{2+} and Mg^{2+} and the anions are generally dominated by HCO_3^+ over SO_4^- and Cl^-.

HZ 2 (122.9–99.0 m)

Both water content and variability are low in this unit (mean: 13 wt%). The stable isotopes are the most depleted of the whole record (at 105.8 m core depth; δ^{18}O min.: −23.0 ‰; δD min.: −176.7 ‰) with low stable isotope variability (δ^{18}O mean: −22.3 ‰; δD mean: −172.1 ‰; *d* excess mean: 6.5 ‰) including a trend towards more negative δ^{18}O and δD values towards the top of the zone. The variability of the slightly basic pH values is low (pH mean: 7.4). This unit is separated from HZ 1 by a small but distinct offset towards lower EC values (EC mean: 55 µS cm^{-1}) and ion load (1.4 meq L^{-1}). The water in HZ 2 is enriched in $Na^+ + K^+$ cations and the anions are dominated by HCO_3^-.

HZ 3 (98.9–36.0 m)

Both water content and variability are low in this unit (mean: 13 wt%) and the stable isotope variations are low overall (δ^{18}O mean: −22.5 ‰; δD mean: −172.1 ‰; *d* excess mean: 7.8 ‰), although the values gently increase towards the upper part of this zone (δ^{18}O max.: −21.6 ‰; δD max.: −166.4 ‰). With little variation pH values are slightly more basic than in the underlying zones (pH mean: 7.7) and the EC values are substantially higher than in the underlying zones (EC mean: 138 µS cm^{-1}), hence the

CPD
9, 3993–4034, 2013

corresponding ion load is higher than in HZs 1 and 2 (up to 3.9 meq L^{-1} at 51.1 m core depth); $Na^+ + K^+$ are again the dominant cations and HCO_3^- is the dominant anion.

HZ 4 (35.9–21.0 m)

Both water content and variability are low in this unit (mean: 15 wt%), the stable isotopic composition gradually becomes heavier from the bottom to the top of this unit ($\delta^{18}O$ mean: −20.0 ‰, $\delta^{18}O$ min.: −21.4 ‰, $\delta^{18}O$ max.: −19.2 ‰; δD mean: −154.2 ‰, δD min.: −164.5 ‰, δD max.: −148.0 ‰), and the *d* excess gradually becomes smaller towards the top of this section (*d* excess mean: 6.0 ‰; *d* excess max.: 7.0 ‰; *d* excess min.: 5.2 ‰); the pH values are less basic than in HZ 3 and are comparable to those in HZ 1 and 2, with little variability (pH mean: 7.4); the EC is lower than in HZ 3 (EC mean: 62 µS cm^{-1}) as is the corresponding ion load (1.3 meq L^{-1}). $Na^+ + K^+$ remain the dominant cations and HCO_3^- the dominant anion.

HZ 5 (20.9–8.0 m)

The water content is low in this unit with slightly greater variability than in the underlying units (mean: 15 wt%, min.: 9 wt%, max.: 22 wt%). Including a distinct break at 13.5 m core depth the stable isotope values increase towards the top of the zone where the heaviest isotope composition of the total record occurs between 11.0 and 8.0 m core depth ($\delta^{18}O$ mean: −18.8 ‰, $\delta^{18}O$ min.: −19.7 ‰, $\delta^{18}O$ max.: −17.2 ‰ ; δD mean: −145.2 ‰, δD min.: −153.2 ‰, δD max: −133.5 ‰), while the *d* excess values decrease towards the top of this zone with a mean of 5.1 ‰ (max.: 7.6 ‰; min.: 2.7 ‰). The pH values are slightly higher and have higher variation than in the underlying zone (pH mean: 7.5; pH min.: 7.0, pH max.: 7.9). The EC values are higher than in the underlying zone and vary to some degree (EC mean: 95, EC min.: 36, EC max.: 207). The corresponding ion load ranges between 0.7 meq L^{-1} (min.) and 5.5 meq L^{-1} (max.) around a mean of 1.7 meq L^{-1}. $Na^+ + K^+$ remain the dominant cations and HCO_3^- the dominant anion.

CPD
9, 3993–4034, 2013

HZ 6 (7.9–5.0 m)

Both water content and variability are low in this unit (mean: 13 wt%), the stable isotopic composition gradually becomes lighter from the bottom to the top of this unit (δ^{18}O mean: −17.5 ‰, δ^{18}O min.: −17.8 ‰, δ^{18}O max: −17.3 ‰; δD mean: −135.2 ‰, δD min.: −137.5 ‰, δD max.: −133.5 ‰), and the *d* excess values decrease (*d* excess mean: 4.7 ‰; *d* excess max.: 5.9; *d* excess min.: 3.4). The pH values are acidic for the first time and show some variability (pH mean: 6.0, pH min.: 5.3, pH max.: 6.9). The EC values are lower than in the underlying zone and show little variability (EC mean: 32 µS cm^{-1}, EC min.: 23 µS cm^{-1}, EC max.: 52 µS cm^{-1}). The corresponding ion load is low (mean: 0.5 meq L^{-1}). $Na^+ + K^+$ remain the dominant cations and HCO_3^- the dominant anion.

HZ 7 (4.9–0.0 m)

The water content of this zone is slightly higher (mean: 16 wt%) than in the underlying zones, including individual layers with water content as high as 45 wt% (i.e. at 1.7 m core depth). The stable isotopic composition is more variable here than in any other zone; it ranges between −21.9 ‰ (δ^{18}O min.) and −17.5 ‰ (δ^{18}O max.) around a mean of −19.8 ‰ (δ^{18}O mean) and between −150.7 ‰ (δD min.) and −170.3 ‰ (δD max.) around a mean of −138.0 ‰ (δD mean). A distinct minimum peak in δ values occurs at 1.7 m core depth, and a maximum peak occurs towards the top of this zone. The *d* excess has the highest value of the total record (+16.6 ‰) at 4.4 m depth following an abrupt transition from the lower values of the underlying HZ 6. Towards the top of HZ 7 the *d* excess values decrease to 1.3 ‰ at 2.1 m depth, before they increase again to 8.3 ‰ at 1.7 m core depth and decrease again (< 2 ‰) in the uppermost meter. The pH values are mostly acidic with little variability (pH mean: 5.9, pH min.: 5.0, pH max: 7.1). The EC values are high (EC mean: 98 µS cm^{-1}) with a distinct maximum peak at 2.0 m core depth (219 µS cm^{-1}) and a minimum peak at 0.4 m core depth (20 µS cm^{-1}). The corresponding ion load ranges around a mean of 0.5 meq L^{-1}

CPD
9, 3993–4034, 2013

with a maximum of 3.7 meq L^{-1} and a minimum of 0.5 meq L^{-1}. $Na^+ + K^+$ remain the dominant cations with the highest proportional amount of all HZs, and whereas in all other zones HCO_3^- was the dominant anion, in HZ 7 SO_4^- is dominant.

5 Discussion

5.1 Ground ice origin: constraints from the ion composition

Based on EC measurements in 2000 and 2003 it was concluded that the lake is mainly fed by melt waters with low ion content as introduced earlier; the specific conductivities in El'gygytgyn Crater inlet streams were all lower than 25 µS cm^{-1} and the lake EC was around 12 µS cm^{-1} (Cremer and Wagner, 2003). Some portions of the ground ice in core 5011-3 come close to this value with EC ~ 50 µS cm^{-1}, i.e. ground ice of HZs 1, 2, 4, 6 (Fig. 3). The other HZs show a higher concentration of light soluble salts with EC values of ~ 100 µS cm^{-1}, i.e. in HZs 3, 5, 7. Water forming the ground ice is mainly of the HCO_3^--($Na^+ + K^+$)-Ca^{2+} type, with the exception of HZ 7, which is SO_4^{2-}-($Na^+ + K^+$) type (Fig. 5). The 5011-3 ground ice may include a lake water component and the contact of the lake water with lake sediments should have altered the hydrochemical properties. The main cations ($Na^+ + K^+$, Ca^{2+}, and Mg^{2+}) likely derive from the interaction with the host rock that builds up the El'gygytgyn Crater and which is the source of the weathered debris in the area. This debris consists of volcanic rocks with rhyolite to andesite composition (Belyi, 1998). There is no inlet to the lake from the outside of the crater; thus, remote sources of the ion load can be excluded. HCO_3^- is estimated to originate mainly from the atmosphere, since carbonate rocks are absent in the area. The small amount of Cl^- may come from the weathering of crystalline rocks (Meybeck, 1987), whereas the sulphate presumably derives from the weathering of local sulphur-bearing minerals (e.g. pyrite), since organic matter contents are low in the core (Schwamborn et al., 2012). Ion activity coefficients are used as a measure of the interaction between the liquid and the solid phase during the process of freezing

CPD
9, 3993–4034, 2013

that forms ground ice. Three binary coefficients of ion activity have been calculated that are related to Ca^{2+} (K^+/Ca^{2+}, Na^+/Ca^{2+}, and Mg^{2+}/Ca^{2+}, Fig. 4). Trends in the ion activity illustrate that for much of the lower ground ice column the relative incorporation of the Na^+ and K^+ cations into the ground ice runs parallel, although the amount of Na^+ (0.16 to 1.17 meq L^{-1}) is commonly 10–20 times greater than the amount of K^+ (0.01 to 0.09 meq L^{-1}). For Mg^{2+} (0.0 to 0.36 meq L^{-1}) a parallel trend is also valid for HZs 1 and 2. A slight offset occurs in HZ 3, where the fraction of Mg^{2+} is relatively higher than that of Na^+ and K^+ in the ground ice. In HZ 4 the variability of Na^+ and K^+ contents increases. In HZs 6 and 7 the variations of Na^+ and K^+ contents are greatest and only in these HZs their relative abundance is higher than that of Mg^{2+}, even though the Mg^{2+} ion has a smaller radius than Na^+ and K^+ (ion radius 10^{-12} m: Mg^{2+} = 72; Ca^{2+} = 100; Na^+ = 102; K^+ = 138). The relative amount of K^+ is highest in HZs 6 and 7. In these upper two zones K^+/Ca^{2+} shows an offset from the otherwise parallel behaviour of Na^+/Ca^{2+}. K^+ is preferentially mobilised during spring thaw (Edwards et al., 1986) and this may point to a source of this cation in the ground ice of HZs 6 and 7. Moreover, the high amounts of K^+ remarkably overlap with the zone of acidic pH in HZs 6 and 7; this acidic pH matches the modern day snow conditions.

Mackay and Lavkulich (1974) report ion concentrations of Cl^-, Mg^{2+}, K^+, Ca^{2+}, and Na^+ in unfrozen water below the permafrost in two drained lakes near Tuktoyaktuk, western Canadian Arctic, to be 10–20 times higher than the concentrations in the surrounding ice. Experiments conducted to assess the effects of salinity on freezing front advance and solute redistribution show that solute exclusion occurs during freezing, resulting in high solute concentration in the unfrozen pore water (Mahar et al., 1983). Kadlec (1984) reports similar observations in peat. These four studies are based on unidirectional freezing, mostly from the surface downward. Although frost penetration in arctic soils mainly takes place from above, additional lateral and upward movement of the freezing front is expected where thawed ground (i.e. talik) below a lake is surrounded by permafrost. This implies that the alternating pattern of higher versus lower ion load as recorded in HZs 7 to 1 combined with the isotope composition mirrors a dif-

CPD
9, 3993–4034, 2013

ferential freezing history for each of the HZs. However, the redistribution of solutes as well as the isotopic composition depend strongly on the freezing rate, moisture content, sediment texture, and time; thus, the proposed scheme of using ion gradients is simplistic. Because many soil surfaces are charged and the solubility of different soil minerals is highly variable and may change through time, ion mobility also depends on the specific ions (Marion, 1995). For example, Ugolini and Anderson (1973) found that Cl^- is more mobile in Antarctic soils than is Na^+, presumably because of the attraction between the negatively charged cation exchange capacity and the positively charged Na^+ ion. Still, a pattern of slow and then more rapid freezing might be inferred from the HZs in core 5011-3. Freezing and ground ice formation in HZs 1–3 presumably took place at a constant rate allowing fairly constant amounts of the main cations to be frozen in, as mirrored in the fairly uniform ion activity record of the HZs 1–3 core portion (Fig. 4). In HZs 4 and 5 the ion pattern becomes more irregular; it exhibits the highest variability in HZs 6 and 7. Here, a more rapid freezing of solute pockets in the active layer likely took place during the time when HZs 6 and 7 formed and may have led to the relative enrichment of K^+ in these HZs. Remarkably, the assumed YD stable isotope peak (as is further discussed below) at 2.5 m depth is associated with a distinct high ion load at the same depth. Previously a similar phenomenon in the P2 record of frozen slope deposits was interpreted as an indication that high ion concentrations in the YD ground ice preserved severe cold-climate weathering (Schwamborn et al., 2008). Possibly the breakdown of sediment particles in the course of seasonal temperature shock and cryogenic weathering (i.e. frost weathering, including ice as a weathering agent, Schwamborn et al., 2012b) increased the total surface area of grains, allowing chemical weathering to become more productive. The individual Cl^- enrichment in the sediment layer at 65.7 m depth is debatable. Possibly a lack of permeability prevented the escape of the solute inclusion from that sediment layer when the layer froze over.

CPD
9, 3993–4034, 2013

5.2 Ground ice origin: constraints from the whole core water stable isotope composition

In the δ^{18}O-δD diagram (Fig. 6) the freezing process causes a deviation from the GMWL along a line with a lower slope (a so-called freezing slope) that can be diagnostic of the conditions prevailing during freezing (Lacelle et al., 2004). During equilibrium freezing, the value of the δ^{18}O-δD regression slope differs from that of the GMWL, because of different isotopic fractionation coefficients (for ^{18}O and D) during the water-ice phase change than is the case for the water-vapour fractionation. The 5011-3 ground ice has a slope of 7.5 suggesting a stable isotope history, which includes kinetic fraction i.e. during freezing, or the impact of the freezing velocity or the inclusion of recycled (i.e. multiple cycles of local evaporation and condensation) water from tundra (Kurita et al., 2003) or open water surfaces in the area. Lately Lacelle (2011) concluded that ice produced by freezing of precipitation or melt water under equilibrium conditions in an open system will tend to have a slope near or greater than 7.3. In contrast, under non-equilibrium conditions an ice body found in Western Canadian Arctic permafrost had a slope of 5.9 and has been interpreted to result from a complete freeze-over of a closed-system water pond in a glacier forefield after the pond had been overridden by paraglacial debris (Fritz et al., 2011).

5.3 Ground ice origin: constraints from downcore hydrochemical and stable isotope variability and sediment data

The pH measurements of the lake water indicate that Lake El'gygytgyn is circumneutral to weakly acidic (Cremer et al., 2005). This is also true for ground ice that was retrieved with two 5 m permafrost cores in the El'gygytgyn Crater (P1 and P2, see Fig. 1) and in nearby ice wedges, which all have weakly acidic pH values between 6 and 7 (Schwamborn et al., 2006). The cores P1 and P2 represent subaerial accumulations of slope deposits and date back to ~ 13 000 yr BP (before present). Similar pH values (5 to 7) are also found in the upper core segments of 5011-3 in HZs 6 and 7. In terms of

CPD
9, 3993–4034, 2013

pH this ground ice portion thus resembles the pH conditions of the modern lake water and near-surface permafrost elsewhere in the crater. Andreev et al. (2012) found that the sediment layers of HZ 6 and 7 are rich in pollen; a typical AD (11.2 to 10.7 ka BP) pollen assemblage is found in the sediment layers between 9.5 and 2.5 m core depth, a Younger Dryas (YD; 10.7 to 10.2 ka BP) pollen association is found between 2.5 and 1.8 m core depth, and a Holocene (10.2 ka BP to modern) pollen composition between 1.8 and 0.0 m core depth (Fig. 2). The warm-climate AD sediment layers correspond to HZ 6, including the prominent maximum peak with the most positive stable isotope composition of the core at 9.0 m core depth (Fig. 4). In contrast, the overlying cold-climate YD sediments show a distinct minimum peak in the ground ice isotope record at 1.8 m core depth, before the second maximum peak with a heavier isotope composition appears in the warm-climate Holocene sediment layers at 0.4 m core depth. δ^{18}O and δD minima and maxima match those of the vegetation change in HZs 6 and 7 layers, and thus sediments likely contain vegetation remains and ground ice evolved from palaeo precipitation of contemporaneous age. This holds true even with the pollen providing a summer signal, whereas the ground ice formed under subaerial conditions is fed by both winter and summer precipitation (Schwamborn et al., 2006). The hydrological history in the HZs 6 and 7 deposits therefore parallels the subaerial sediment history. When excluding a lake origin of the ground ice in HZ 7 the isotopic composition of HZ 7 is similar to the one for snow with both groups having similar mean δ values. HZ 6 is shifted towards higher mean δ values, falling between the isotopic composition of rain and snow. Similar overlapping histories of synsedimentary ground ice formation where palaeo precipitation changes are paralleled by bio indicators during the late Quaternary are known from other terrestrial permafrost archives in Northern Siberia (e.g. Schirrmeister et al., 2003; Wetterich et al., 2011; Vasil'chuk et al., 2012).

The varying *d* excess values in HZs 6 and 7 ranging between more than 16 ‰ and 1 ‰ (Fig. 4) indicate that during the formation time the ground ice likely was frozen and thawed various times with the palaeo precipitation signal still being preserved. Decreasing *d* excess may be related to greater input from rain rather than snow into

CPD
9, 3993–4034, 2013

the ground ice system, because rain may be influenced by secondary evaporation and by the recycling of regional moisture in the tundra (Kurita et al., 2003). Especially in the uppermost 5 m of core (HZ 7), secondary fractionation can be detected with δ values above the GMWL (Fig. 6). At least one event of thermal change during the late Holocene is also seen in changes of diatom associations found in Lake El'gygytgyn sediments. They demonstrate that at about 3.6 ka BP summers warmed, resulting in longer ice-free seasons and higher bio productivity in the lake (Cremer and Wagner, 2003). On the land surface this coincides with the transition from the formation of a lower to the formation of an upper ice wedge generation in slope deposits of the El'gygytgyn Crater (Schwamborn et al., 2006). Hence, likely a precipitation signal changed by kinetic fractionation has been preserved in the ground ice of the slope deposits back to the AD and subaerial slope deposits have accumulated at the 5011-3 coring site since that time. For comparison, thermal change across the AD-YD-Holocene transition as expressed in increasing d excess from 3 ‰ to 10 ‰ is known from an Alaska near surface ground ice formation fed by palaeo precipitation (Meyer et al., 2010).

In contrast, the weakly basic pH found from HZs 1 to 5 (pH between 7 and 8, Fig. 3) differs from that of HZs 6 and 7 with its subaerial signature and points to a different ground ice genesis. Depending on core depth and the HZ zonation under consideration, the stable isotope composition of the ground ice has different overlaps with the compositions of other water types sampled in the area (Table 1, Fig. 7). The $\delta^{18}O$ mean values of snow and lake water (−19.8 ‰) in the El'gygytgyn Crater are similar and suggest that the lake water composition is largely controlled by snow. Earlier it was stated that the lake is snowmelt fed (Cremer and Wagner, 2003) based on the low lake water EC ($< 20\,\mu S\,cm^{-1}$). In recent studies it was found that the lake water column is well mixed with low evaporation (Chapligin et al., 2012) and the period of lake water residence time is about 100 yr (Fedorov et al., 2012). An isotopic composition similar to what has been described for snow and lake water is found in particular in HZ 4 with their matching mean δ values (Fig. 7).

CPD
9, 3993–4034, 2013

The stable isotope composition of HZ 5 is similar to the isotopic composition of stream input with slightly higher δ values. Wilkie et al. (2013) have specified an annual average partitioning of precipitation in El'gygytgyn Crater into 60 % winter contribution and 40 % summer input (annual average $\delta^{18}O = -19.3$ ‰, $\delta D = -152.9$ ‰). Bearing in mind this estimate and also the error bars of minimum and maximum δ values in the sample sets (Table 1, Fig. 7), the possibility that rain input has influenced the formation of 5011-3 ground ice cannot be ruled out. Similarly, from the subaerial ground ice formations found in cores P1 and P2 (Fig. 7) a two-component snow and rain input mixture has been suggested; if the mean snow and mean rain isotopic composition are considered as the two end members, the relative proportions would be 89 ‰ snow and 11 % rain when using $\delta^{18}O$, and 84 % snow and 16 % rain if using δD for the mixing calculations (Schwamborn et al., 2006). The isotopic composition of lake ice and streams are slightly more positive than the lake water by 1.4 ‰ and 0.9 ‰, respectively, and demonstrate that the first ice to form in autumn and the first melt water to run off in spring is enriched in ^{18}O isotopes compared to lake water.

The isotopic composition of HZs 1, 2, and 3 is similar to the one of ice wedges, especially ice wedges from the Late Holocene (Fig. 7). Those ice wedges formed on subaerial slopes in the crater (Schwamborn et al., 2006) and are mainly fed by early spring snow melt water (Lachenbruch, 1962). There is no indication that ice wedge formations have been extracted with core 5011-3 and if the ground ice in HZs 1, 2, and 3 evolved from lake water freezing instead, this would argue for colder temperatures during ground ice development, since HZs 1, 2, and 3 exhibit the lowest δ values ($\delta^{18}O$ min.: −23 ‰; δD min.: −180 ‰) found in the 5011-3 ground ice record. Thus, at that time the lake and the precipitation feeding it must have had considerably more negative δ values than at present, indicating environmental conditions typical of cold-climate periods. The downcore records of $\delta^{18}O$ and δD from HZs 1 to 3 exhibit fairly uniform values ($\delta^{18}O$ around −22 ‰; $\delta^{18}O$ around −170 ‰) and the combination of little isotope content variation and a stable *d* excess in HZs 1 to 3 points to a constant freezing rate of the host water in an open system (i.e. connected to the water source).

CPD
9, 3993–4034, 2013

In HZ 4 the δ values are 4 ‰ more positive than in HZs 1 to 3, and in combination with a slightly decreasing d excess from 8 ‰ to 6 ‰ this suggests either different host water or a different mode of freezing when compared with the underlying zones. The same is true for the upper part of HZ 5, which is more positive by 2 ‰ in $\delta^{18}O$. It also exhibits a continuing d excess decrease to 4 ‰. The rather linear trend of decreasing d excess can be traced between 50 m and 8 m core depth, whereby the δ values show two rhythmic increases; the first one between 50 m and 30 m core depth (in HZs 3 and 4), and the second one between 18 m and 8 m core depth (in HZ 5). The maximum δ values occur at 8 m core depth accompanied by a d excess minimum. Consequently, freezing likely took place in at least two stages with a freezing front likely migrating from top to down and leading to an isotopically more heavy ground ice in the layers, which froze over first.

5.4 Interpretation based on permafrost and lake dynamics

When combining the sediment description and the pollen load of 5011-3 it was concluded that the coring site, which is exposed today, was flooded during times of higher lake levels for at least two periods in the Quaternary. There are two sets of prominent sandy horizons in core 5011-3, between 24.0 and 19.0 m and between 9.6 and 9.1 m core depth. These sandy horizons have been interpreted to represent two flooding events (Schwamborn et al., 2012). The lower sandy beds presumably formed during marine isotope stage (MIS) 7 according to an age estimate based on the pollen load (Andreev et al., 2012). Tentatively the associated relative lake level high at that time is linked to the "Middle Pleistocene" shoreline (+40 m terrace) as described by Glushkova and Smirnov (2007).

A second ancient shoreline is interpreted from shoreline remnants that can be found at 11–9 m above the present lake level (+10 m terrace) at the southern bluffs of the lake (Glushkova and Smirnov, 2007). Based on tree pollen counts (i.e. especially *Pinus*) the pollen assemblage is similar to those in MIS 5 layers of lake core 5011-1 (A. Andreev, personal communication, 2013), whereby the uppermost three meters show a similarity

CPD
9, 3993–4034, 2013

with the MIS 4 pollen stratigraphy of the lake cores. In permafrost core 5011-3 there are no corresponding lake deposits that have preserved evidence of this relatively high lake level. Possibly those sediments were removed by erosion on the slope. However, preservation of a lake level highstand in the 5011-3 permafrost record due to thaw and freeze of the ground ice in the course of flooding and a subsequent lake shore retreat can be assumed.

During the LGM the lake level was 10 to 12 m lower (−10 m terrace) than the modern level (Juschus et al., 2011) and thus site 5011-3 was exposed. A temperature profile of borehole 5011-3 suggests that the permafrost around the lake has inherited the temperature field from that time, since the minimum temperatures below the zone of seasonal variation are lower than can be generated by modern day conditions. Based on forward modelling Mottaghy et al. (2013) explained a temperature minimum of −6.7 °C at 60 m borehole depth as the result of much deeper permafrost at the end of the LGM (Fig. 8). The amplitude of the LGM and the following warming from the Late Pleistocene to the Holocene has influenced the temperature distribution at all depths up to the surface. This means that the low LGM temperatures have overprinted any temperature history from, for example, the MIS 7 flooding event that warmed the ground at that time. On the other hand, ground warming during the AD and the Holocene did not erase the transient LGM temperature distribution and thus reached a depth less than 60 m.

The AD age of the upper sandy beds (9.6 to 9.1 m core depth) in 5011-3 has been estimated from the pollen load (Andreev et al., 2012) and is compatible with a reconstructed lake level 3 to 4 m higher than modern (+4 m terrace) during that time (Schwamborn et al., 2008). After the AD flooding event the lake level dropped again and the deposits froze over. The topmost 9.1 m in the core represent slope deposits and creek fill from the AD to modern day, where migrating creeks reworked and distributed coarse-grained slope material (i.e. gravelly sand) and prograded into the lake.

If we accept the interpretation of at least three flooding events that reached the coring site during MIS 7, MIS 5, and the AD, a talik formation should have been induced at

CPD
9, 3993–4034, 2013

these times by the thermal heat flow from the water column on top of the permafrost soil of that time. For comparison, a 7000 yr old Lena Delta thermokarst lake is known to have developed a talik about 90 m thick below a water depth of about 10 m in a fine sandy substrate (Schwamborn et al., 2002). This study was based on seismic profiling, sediment coring, and modelling. Based on modelling results Ling and Zhang (2003) expect a talik extension at a site in Alaska to take place within 3000 yr with a maximum downward depth of 53.2 m after the formation of a shallow thaw lake with a long-term mean lake bottom temperature of 3.0 °C. Lake El'gygytgyn is similar to that; it has a measured temperature between 3 and 4 °C at the bottom depending on the season (Cremer and Wagner, 2003). Thus time and depth dimensions of those two other sites are comparable with Lake El'gygytgyn when considering past talik growth at the lake edge.

Based on the hydrochemical zonation of the ground ice we postulate talik development and subsequent refreezing as illustrated in Figs. 8 and 9. The proposed scheme includes that more recent environmental change might have erased older signatures in the hydrochemical record. Presently the lake level is 8 m lower than the coring site and thus HZs 7 and 6 reflect the subaerial situation. The low pH is typical for meteoric water and the varying EC and ion content and activity changes reflect site-specific rapid freezing processes in the subaerial slope deposits. The ground ice isotopes exhibit maximum $\delta^{18}O$ values of −17 ‰ in the uppermost two core meters and in the bottom of HZ 6 indicating relatively warm conditions at these times. HZ 7 is interrupted by a minimum $\delta^{18}O$ value of −21.9 ‰ at 1.8 m core depth, which points to significantly colder conditions during the YD. This is confirmed by the pollen composition and supported by a relative maximum in ion content; the high EC points to greater physical break-up of rock fragments, which may have increased the surface for chemical weathering. Both climatic trends (i.e. cooling from AD to YD, warming from YD to Holocene) are still visible despite variable *d* excess. The variable *d* excess illustrates that the ground ice formation has not evolved directly from original precipitation water, but likely

CPD
9, 3993–4034, 2013

has undergone post-depositional fractionation in the course of seasonal freezing and thawing of active layer material on the slope.

At the top level of HZ 5 a set of sand layers are interpreted to have connected with a former lake terrace dated to AD times. Consequently the AD lake water reached this level and the lake water body's latent heat potentially impacted the underlying sediments. The $\delta^{18}O$ decrease from −17 ‰ to −19 ‰ between 9.0 m and 15.0 m core depth may indicate a freezing process from the top to the bottom, which is attributed to Rayleigh fractionation during freezing of water, as the heavy isotopes (^{18}O and D) are preferentially incorporated into the solid phase first (Lacelle, 2011).

The AD flooding was possibly a short-term event with talik expansion that did not reach deeper than about 5 m; i.e. only the core section between 9.6 m and 15 m core depth is affected (Fig. 8). Below 15 m core depth the section is likely connected to a refreezing of sediment layers, which were thawed during an earlier lake level high, presumably during the MIS 5, when the +10 m terrace marked the lake level and the coring site was also inundated. Likewise, high pH values mark the freezing process in HZ 5, when H^+ ions may have been expelled from the water when the freezing front migrated through the sediments. The decreasing ion concentration from the top to the bottom in HZ 5 suggests that the freezing front likely migrated from the top to the bottom, expelling more ions in the bottom layers where the freezing process was less rapid than in the upper layers.

At the top level of HZ 4 the sand layer is interpreted as former lake sediments dated to MIS 7. Consequently, MIS 7 lake water reached this level and the lake water body's latent heat potentially impacted underlying sediments. The low ion content demonstrates that this section down to 36 m core depth likely was affected twice by thawing and refreezing of the deposits; by the MIS 7 relative lake level high stand, associated talik formation, and subsequent freezing when the lake level lowered, and also by the MIS 5 high stand with similar thaw and freeze back dynamics. A possible strong precipitation signal in the stable isotope composition of the ground ice in the subaerial slope deposits, which might have accumulated after the MIS 7 lake level high stand

CPD
9, 3993–4034, 2013

and before the MIS 5 lake level high stand, may have been erased from the record in the course of the thawing induced by the MIS 5 flooding. During the flooding events and talik formation there was potentially a lateral contact between the talik and the lake water.

In HZ 3 δ^{18}O decreases from −19 ‰ to −22 ‰. Along with the tendency of lighter isotope composition towards the bottom, this may again indicate that freezing occurred from top to bottom as introduced earlier. High pH and EC, and constant isotope composition both in δ values (δ^{18}O very light: −23 ‰ to −24 ‰) and d excess (8 ‰) below approx. 50 m core depth suggest a relatively uniform water body. The low δ^{18}O values may be the result of a Rayleigh-type isotope fractionation between water and ice under equilibrium conditions. The low δ^{18}O composition in HZ 3 may thus be explained by slow freezing with a lateral contact to the lake and the low variability in d excess may be produced by a freezing front that migrated horizontally through the sediments. The high EC content points to lake water that had possibly received a greater load of light soluble salts from increased chemical weathering. Alternatively it cannot be ruled out that the inclusion of a greater ion load must be closely linked to the freezing dynamics along the approaching freezing front at that time. This would however contradict Qiu's statement that especially in freezing sandy environments the solutes migrate to the unfrozen zone (Qiu et al., 1988).

A similar scenario is suggested for HZs 1 and 2. The stable isotope composition and a d excess of 7 ‰ is nearly the same as in HZ 3, but the EC content of the ground ice is distinctly lower. The EC separates HZs 1 and 2 from HZ 3 and also from each other, thus pointing to separate freezing histories of separate host waters prior to HZ 3 ground ice formation.

According to the interpretation of changing lake levels through time talik development, migration, and refreezing in the lake margin should have taken place. From that viewpoint the talik development associated with the MIS 7 lake level existed for a longer period of time, since the hydrochemical zonation indicates a thaw bulb that extended deeply. Given that the heat capacity and thermal conductivity in the sandy gravel is

CPD
9, 3993–4034, 2013

fairly uniform, the MIS 7 talik reaches from the flooding horizon at 19.0 m down to 101.0 m core depth, the base of HZ 3. The relatively low δ values of the stable isotope composition in HZ 3 might be explained by the ancient Lake El'gygytgyn waters; possibly the water at that time exhibited fairly negative isotopic composition, and a slow and uniform freezing process from the side in an open system led to homogeneous fractionation. After the lake level lowered following the MIS 7 flooding, subaerial slope deposits presumably overrode the HZ 4 layers and the talik refroze in the course of surface cooling.

Analogously, the ground ice of HZs 2 and 1 may have developed in the course of ancient talik thaw-and-freeze. The combination of little variation of the isotope content and a little variation of the ion load suggests that the ground ice developed similarly in both HZ 2 and 1 by freezing out of a uniform water body, possibly from lake water. This should have occurred prior to MIS 7 talik, which affected the overlying sediments, but there is no ancient lake level reconstruction available for that time to support a more detailed interpretation. Any interpretation may become more difficult, if it attempts to link the negative δ values (i.e. δ^{18}O at −22 ‰ to −23 ‰) to an interglacial high lake level, as is the case with the other reconstructed lake levels. The modern lake water isotope composition of δ^{18}O = −19.3 ‰ is characteristic of a warm period, but the LGM, the most pronounced cold period in the past 250 000 yr, has a deduced δ^{18}O = −21.0 ‰ (Chapligin et al., 2012b).

6 Conclusions

A 141 m long ground ice record from the permafrost margin of Lake El'gygytgyn allows a complex history of thaw-and-freeze to be reconstructed in the course of Quaternary flooding events at the lake edge.

Zones of low variability in stable water isotope composition are interpreted to result from refreezing of former talik zones and zones of high variability in ion content point to a comparatively rapid top-down freezing process.

CPD
9, 3993–4034, 2013

The following is concluded from the interpretation of the ground ice hydrochemical data from the studied 141 m long permafrost core 5011-3:

Ground ice of precipitation origin is preserved in the upper 9.6 m of core. The palaeoclimate record includes ground ice formation from the AD, the YD, and the Holocene; it matches the principal climate history of the Eurasian Arctic during that time and is mirrored by the pollen stratigraphy of the sediment layers.

The record between 141.0 and 9.6 m core depth has evolved from postdepositional thawing, including partial mixing with lake water from the neighbouring Lake El'gygytgyn in the course of lake flooding events. The isotope compositions represent lake water, which has been overprinted by the refreezing talik.

At least three cycles of talik development and subsequent refreezing can be reconstructed based on known lake level fluctuations: a MIS 7 refrozen talik between 101 m and 19 m core depth, a refrozen MIS 5 talik between 36 m and 15 m core depth, and a refrozen AD talik between 15 m and 9.6 m core depth. Two more cycles of talik refreezing may be represented in the bottom part of the core (i.e. at 141–124 m and 124–101 m core depth). However, at present they cannot be linked to known ancient lake level high stands, but likely have inherited strong isotope fractionation histories.

Past thaw and freeze in the lake marginal area likely has destabilised the slope and is considered a cause of frequent sliding events, as evidenced by mass movement deposits in lake core 5011-1. Further discussion of the sedimentation processes in the deeper basin of Lake El'gygytgyn and the glacial versus interglacial turbidite record of core 5011-1 can be found in Sauerbrey et al. (2013).

Acknowledgements. Funding for this research was provided by the ICDP, the US National Science Foundation (NSF), the German Federal Ministry of Education and Research (BMBF), the Alfred Wegener Institute, Helmholtz Centre for Polar and Marine Research (AWI) and GeoForschungsZentrum Potsdam (GFZ), the Russian Academy of Sciences Far East Branch (RAS FEB), the Russian Foundation for Basic Research (RFBR), and the Austrian Federal Ministry of Science and Research (BMWF). A Russian mining rig (SIF-650M) was employed by Sergey Gutov and his crew from a local drilling company (Chaun Mining Corp., Pevek). Partic-

CPD
9, 3993–4034, 2013

ular thanks go to Bernhard Chapligin and Nikifor Ostanin for help in the field. The lab support by Antje Eulenburg and Ute Bastian is highly appreciated.

References

Andreev, A. A., Morozova, E., Fedorov, G., Schirrmeister, L., Bobrov, A. A., Kienast, F., and Schwamborn, G.: Vegetation history of central Chukotka deduced from permafrost paleoenvironmental records of the El'gygytgyn Impact Crater, Clim. Past, 8, 1287–1300, doi:10.5194/cp-8-1287-2012, 2012.

Belyi, V. F.: Impactogenesis and volcanism of the El'gygytgyn depression, Petrology, 6, 86–99, 1998.

Brigham-Grette, J., Melles, M., Minyuk, P., Andreev, A., Tarasov, P., DeConto, R., Koenig, S., Nowaczyk, N., Wennrich, V., Rosén, P., Haltia, E., Cook, T., Gebhardt, C., Meyer-Jacob, C., Snyder, J., and Herzschuh, U.: Pliocene Warmth, polar amplification, and stepped pleistocene cooling recorded in NE Arctic Russia, Science, 340, 1421–1427, doi:10.1126/science.1233137, 2013.

Chapligin, B., Meyer, H., Bryan, A., Snyder, J., and Kemnitz, H.: Assessment of purification and contamination correction methods for analysing the oxygen isotope composition from biogenic silica, Chem. Geol., 300–301, 185–199, 2012a.

Chapligin, B., Meyer, H., Swann, G. E. A., Meyer-Jacob, C., and Hubberten, H.-W.: A 250 ka oxygen isotope record from diatoms at Lake El'gygytgyn, far east Russian Arctic, Clim. Past, 8, 1621–1636, doi:10.5194/cp-8-1621-2012, 2012b.

Craig, H.: Isotopic variations in meteoric waters, Science, 133, 1702–1703, 1961.

Cremer, H. and Wagner, B.: The diatom flora in the ultra-oligotrophic Lake El'gygytgyn, Chukotka, Polar Biol., 26, 105–114, 2003.

Cremer, H., Wagner, B., Juschus, O., and Melles, M.: A microscopical study of diatom phytoplankton in deep crater Lake El'gygytgyn, northeast Siberia, Algolog. Stud., 116, 147–169, doi:10.1127/1864-1318/2005/0116-0147, 2005.

Dansgaard, W.: Stable isotopes in precipitation, Tellus, 16, 4, 436–468, 1964.

Dereviagin, A.Yu., Chizhov, A. B., Meyer, H., Hubberten, H.-W., and Siegert, Ch.: Recent ground ice and its formation on evidence of isotopic analysis, in: Proceedings of 8th In-

CPD
9, 3993–4034, 2013

ternational Conference on Permafrost, 21–25 July 2003, Zurich, Switzerland, 5809–5827, 2003.
Edwards, A. C., Creasey, J., and Cresser, M. S.: Soil freezing effects on upland stream solute chemistry, Water Res., 20, 831–834, 1986.
Fedorov, G., Nolan, M., Brigham-Grette, J., Bolshiyanov, D., Schwamborn, G., and Juschus, O.: Lake El'gygytgyn water and sediment balance components overview and its implications for the sedimentary record, Clim. Past Discuss., 8, 3977–4001, doi:10.5194/cpd-8-3977-2012, 2012.
Fritz, M., Wetterich, S., Meyer, H., Schirrmeister, L., Lantuit, H., and Pollard, W. H.: Origin and characteristics of massive ground ice on Herschel Island (western Canadian Arctic) as revealed by stable water isotope and Hydrochemical signatures, Permafrost Periglac. Process., 22, 26–38, doi:10.1002/ppp.714, 2011.
Glushkova, O. Yu. and Smirnov, V. N.: Pliocene to Holocene geomorphic evolution and paleogeography of the Elgygytgyn Lake region, NE Russia, J. Paleolimnol., 37, 37–47, 2007.
Hallet, B.: Solute distribution in freezing ground, in: Proc. 3rd Int. Conf. Permafrost, 10–13 July 1978, Vol. I, National Research Council of Canada, Ottawa, Ontario, 85–91, 1978.
Juschus, O., Melles, M., Gebhardt, C., and Niessen, F.: Late Quaternary mass movement events in Lake El'gygytgyn, northeastern Siberia, Sedimentology, 56, 2155–2174, 2009.
Juschus, O., Pavlov, M., Schwamborn, G., Preusser, F., Fedorov, G., and Melles, M.: Late Quaternary lake-level changes of Lake El'gygytgyn, NE Siberia, Quaternary Res., 76, 441–451, 2011.
Kokelj, S. V. and Burn, C.: Geochemistry of the active layer and near-surface permafrost, Mackenzie delta region, northwest territories, Canada, Can. J. Earth Sci., 42, 37–48, 2005.
Kurita, N., Numaguti, A., Sugimoto, A., Ichiyanagi, K., and Yoshida, N.: Relationship between the variation of isotopic ratios and the source of summer precipitation in eastern Siberia, J. Geophys. Res., 108, 4339, doi:10.1029/2001JD001359, 2003.
Lacelle, D.: On the $\delta^{18}O$, δD and D-excess relations in meteoric precipitation and during equilibrium freezing: theoretical approach and field examples, Permafrost Periglac., 22, 13–25, doi:10.1002/ppp.712, 2011.
Lacelle, D., Bjornson, J., Lauriol, B., Clark, I. D., and Troutet, Y.: Segregated-intrusive ice of subglacial meltwater origin in retrogressive thaw flow headwalls, Richardson Mountains, N. W. T., Canada, Quaternary Sci. Rev., 23, 681–696, 2004.

CPD
9, 3993–4034, 2013

Lacelle, D., St-Jean, M., Lauriol, B., Clark, I. D., Lewkowicz, A., Froese, D. G., Kuehn, S. C., and Zazula, G.: Burial and preservation of a 30 000 yr old perennial snowbank in Red Creek valley, Ogilvie Mountains, central Yukon, Canada, Quaternary Sci. Rev., 28, 3401–3413, 2009.
Lachenbruch, A. H.: Mechanics of thermal contraction cracks and ice-wedge polygons in permafrost, The Geological Society of America, Special papers GSA, 70, 1–69, 1962.
Layer, P. W.: Argon-40/argon-39 age of the El'gygytgyn impact event, Chukotka, Russia, Meteor. Planet. Sci., 35, 581–599, 2000.
Leibman, M. O.: Results of chemical testing for various types of water and ice, Yamal Peninsula, Russia, Permafrost Periglac., 7, 287–296, 1996.
Ling, F. and Zhang, T.: Numerical simulation of permafrost thermal regime and talik development under shallow thaw lakes on the Alaskan Arctic Coastal Plain, J. Geophys. Res., 108, 4511, doi:10.1029/2002JD003014, 2003.
Mackay, J. R.: Oxygen isotope variations in permafrost, Tuktoyaktuk peninsula area, Northwest Territories, Geol. Surv. Can. Paper, 83, 67–74, 1983.
Mackay, J. R.: Pingo Growth and collapse, Tuktoyaktuk Peninsula area, western Arctic Coast, Canada: a long-term field study, Geogr. Phys. Quatern., 52, 271–323, 1998.
Mackay, J. R. and Lavkulich, L. M.: Ionic and oxygen isotopic fractionation in permafrost growth, Geol. Surv. Can. Paper, 74, 255–256, 1974.
Mahar, L. J., Wilson, R. M., and Vinson, T. S.: Physical and numerical modeling of uniaxial freezing in saline gravel, in: Proc. 4th Int. Conf. Permafrost, Nat. Acad. Press, Washington DC, USA, 773–778, 1983.
Marion, G. M.: Freeze-thaw processes and soil chemistry, Special Report 95-12, US Army Cold Regions Research and Engineering Laboratory, 72 Lyme Road, Hanover, New Hampshire, 1–23, 1995.
Melles, M., Brigham-Grette, J., Minyuk, P. S., Nowaczyk, N.R, Wennrich, V., DeConto, R. M., Anderson, P. A., Andreev, A. A., Coletti, A., Cook, T. L., Haltia-Hovi, E., Kukkonen, M., Lozhkin, A. V., Rosén, P., Tarasov, P. E., Vogel, H., and Wagner, B.: 2.8 million years of Arctic climate change from Lake El'gygytgyn, NE Russia, Science, 307, 315–310, doi:10.1126/science.1222135, 2012.
Meybeck, M.: Global chemical weathering of surficial rocks estimated from river dissolved loads, Am. J. Sci., 287, 401–428, 1987.

CPD
9, 3993–4034, 2013

Meyer, H., Schönicke, L., Wand, U., Hubberten, H.-W., and Friedrichsen, H.: Isotope studies of hydrogen and oxygen in ground ice: experiences with the equilibration technique, Isot. Environ. Healt. S., 36, 133–149, 2000.

Meyer, H., Siegert, C., Derevyagin, A., Schirrmeister, L., and Hubberten, H.-W.: Paleoclimate reconstruction on Big Lyakhovsky Island, North Siberia – hydrogen and oxygen isotopes in ice wedges, Permafrost Periglac., 13, 91–103, 2002a.

Meyer, H., Dereviagin, A.Yu., Siegert, C., and Hubberten, H.-W.: Paleoclimate studies on Bykovsky Peninsula, North Siberia – hydrogen and oxygen isotopes in ground ice, Polarforschung, 70, 37–51, 2002b.

Meyer, H., Schirrmeister, L., Yoshikawa, K., Opel, T., Wetterich, S., Hubberten, H.-W., and Brown, J.: Permafrost evidence for severe winter cooling during the Younger Dryas in northern Alaska, Geophys. Res. Lett., 37, L03501, doi:10.1029/2009GL041013, 2010a.

Meyer, H., Schirrmeister, L., Andreev, A., Wagner, D., Hubberten, H.-W., Yoshikawa, K., Bobrov, A., Wetterich, S., Opel, T., Kandiano, E., and Brown, J.: Late Glacial and Holocene isotopic and environmental history of northern coastal Alaska results from a buried ice-wedge system at Barrow, Quaternary Sci. Rev., 29, 3720–3735, 2010b.

Michel, F. A.: Isotope characterisation of ground ice in northern Canada, Permafrost Periglac., 22, 3–12, 2011.

Mottaghy, D., Schwamborn, G., and Rath, V.: Past climate changes and permafrost depth at the Lake El'gygytgyn site: implications from data and thermal modeling, Clim. Past, 9, 119–133, doi:10.5194/cp-9-119-2013, 2013.

Niessen, F., Gebhardt, C. A., Kopsch, C., and Wagner, B.: Seismic investigation of the El'gygytgyn Impact Crater Lake, Central Chukotka, NE Siberia, Preliminary results, J. Paleolimnol., 37, 49–63, 2007.

Nolan, M. and Brigham-Grette, J.: Basic hydrology, limnology, and meteorology of modern Lake El'gygytgyn, Siberia, J. Paleolimnol., 37, 17–35, 2007.

Opel, T., Derevyagin, A. Y., Meyer, H., Schirrmeister, L., and Wetterich, S.: Paleoclimatic information from stable water isotopes of Holocene ice wedges on the Dmitrii Laptev Strait, Northeast Siberia, Russia, Permafrost Periglac., 22, 84–100, 2011.

Ostroumov, V., Siegert, Ch., Alekseev, A., Demidov, V., and Alekseeva, T.: Permafrost as a frozen geochemical barrier, in: Proc. 7th Int. Conf. on Permafrost, Yellowknife, June 1998, edited by: Lewkowicz, A. G. and Allard, M., 855–859, 1998.

CPD
9, 3993–4034, 2013

Ostroumov, V., Hoover, R., Ostroumova, N., Van Vliet-Lanoë, B., Siegert, Ch., and Sorokovikov, V.: Redistribution of soluble components during ice segregation in freezing ground, Cold Reg. Sci. Technol., 32, 175–182, 2001.

O'Sullivan, J. B.: Geochemistry of Permafrost: Barrow, Alaska, in: Proc. Intern. Conf. Permafrost, 11–15 November 1963, Lafayette, Indiana, Natl. Acad. Science, Washington DC, 30–37, 1963.

Qiu, G., Sheng, W., Huang, C., and Zheng, K.: Direction of ion migration during cooling and freezing processes, in: Proc. Fifth Int. Conf. Permafrost, Trondheim, Norway, August 1988, 442–447, 1988.

Rozanski, K., Araguás-Araguás, L., and Gonfiantini, R.: Isotopic patterns in modern global precipitation, in: Climate Change in Continental Isotopic Records, Geophys. Monogr. Ser., 78, edited by: Swart, P. K., Lohmann, K. C., McKenzie, J., and Savin, S., AGU, Washington, DC, 1–36, doi:10.1029/GM078p0001, 1993.

Sauerbrey, M. A., Juschus, O., Gebhardt, A. C., Wennrich, V., Nowaczyk, N. R., and Melles, M.: Mass movement deposits in the 3.6 Ma sediment record of Lake El'gygytgyn, Far East Russian Arctic: classification, distribution and preliminary interpretation, Clim. Past Discuss., 9, 467–505, doi:10.5194/cpd-9-467-2013, 2013.

Schirrmeister, L., Siegert, C., Kuznetsova, T., Kuzmina, S., Andreev, A. A., Kienast, F., Meyer, H., and Bobrov, A.: Paleoenvironmental and paleoclimatic records from permafrost deposits in the Arctic region of Northern Siberia, Quatern. Int., 89, 97–118, 2002.

Schirrmeister, L., Grosse, G., Schwamborn, G., Andreev, A. A., Meyer, H., Kunitsky, V. V., Kuznetsova, T. V., Dorozhkina, M. V., Pavlova, E. Y., Bobrov, A. A., and Oezen, D.: Late Quaternary history of the accumulation plain north of the Chekanovsky Ridge (Lena Delta, Russia): a multidisciplinary approach, Polar Geography, 27, 277–319, 2003.

Schwamborn, G., Andreev, A., Rachold, V., Hubberten, H.-W., Grigoriev, M. N., Tumskoy, V., Pavlova, E. Y., and Dorozhkina, M. V.: Evolution of Lake Nikolay, Arga Island, western Lena River delta, during Late Pleistocene and Holocene time, Polarforschung, 70, 69–82, 2002.

Schwamborn, G., Meyer, H., Fedorov, G., Schirrmeister, L., and Hubberten, H.-W.: Ground ice and slope sediments archiving Late Quaternary paleoenvironment and paleoclimate signals at the margins of El'gygytgyn Crater, NE Siberia, Quaternary Res., 66, 2, 259–272, 2006.

Schwamborn, G., Fedorov, G., Schirrmeister, L., Meyer, H., and Hubberten, H.-W.: Periglacial sediment variations controlled by Late Quaternary climate and lake level rise at El'gygytgyn Crater, Arctic Siberia, Boreas, 37, 55–65, 2008.

CPD
9, 3993–4034, 2013

Schwamborn, G., Fedorov, G., Ostanin, N., Schirrmeister, L., Andreev, A., and the El'gygytgyn Scientific Party: Depositional dynamics in the El'gygytgyn Crater margin: implications for the 3.6 Ma old sediment archive, Clim. Past, 8, 1897–1911, doi:10.5194/cp-8-1897-2012, 2012a.

Schwamborn, G., Schirrmeister, L., Fruütsch, F., and Diekmann, B.: Quartz weathering in freeze–thaw cycles: experiment and application to the El'gygytgyn Crater Lake record for tracing Siberian permafrost history, Geogr. Ann. A, 94, 481–499, doi:10.1111/j.1468-0459.2012.00472.x, 2012b.

Seeberg-Elverfeldt, J., Schlüter, M., Feseker, T., and Kölling, M.: Rhizon sampling of pore waters near the sediment/water interface of aquatic systems, Limnol. Oceanogr., 3, 361–371, 2005.

Souchez, R. A., Jouzel, J., Lorrain, R., Sleewaegen, S., Stiévenard, M., and Verbeke, V.: A kinetic isotope effect during ice formation by water freezing, Geophys. Res. Lett., 27, 1923–1926, 2000.

Stuiver, M. and Yang, I. C.: Oxygen isotope ratios of Antarctic permafrost and glacier ice, in: Antarctic Research Series 33, Dry Valley Drilling Project, American Geophysical Union, Washington, D.C., 131–139, 1981.

Swanger, K. M., Marchant, D. R., Kowalewski, D. E., and Head, J. W.: Viscous flow lobes in central Taylor Valley, Antarctica: origin as remnant buried glacial ice, Geomorphology, 120, 174–185, 2010.

Ugolini, E. C. and Anderson, D. M.: Ionic migration and weathering in frozen Antarctic soils, Soil Sci., 115, 461–470, 1973.

Vasil'chuk, Yu. K., Vasil'chuk, A. C., and Budantseva, N. A.: Isotopic and palynological compositions of a massive ice in the Mordyyakha River, Central Yamal Peninsula, Dokl. Earth Sci., 446, 1105–1109, 2012.

Wetterich, S., Rudaya, N., Tumskoy, V., Andreev, A. A., Opel, T., Schirrmeister, L., and Meyer, H.: Last Glacial Maximum records in permafrost of the East Siberian Arctic, Quaternary Sci. Rev., 30, 3139–3151, 2011.

Wilkie, K. M. K., Chapligin, B., Meyer, H., Burns, S., Petsch, S., and Brigham-Grette, J.: Modern isotope hydrology and controls on δD of plant leaf waxes at Lake El'gygytgyn, NE Russia, Clim. Past, 9, 335–352, doi:10.5194/cp-9-335-2013, 2013.

CPD
9, 3993–4034, 2013

Table 1. Mean values and range ($\delta^{18}O$, δD, d excess) for H_2O sample sets of pore ice, precipitation, and surface waters.

H_2O sample sets	$\delta^{18}O$ (‰) vs. VSMOW	δD (‰) vs. VSMOW	d excess (‰)
pore ice HZ 7 core 5011-3 (n = 18)	−19.9 (−21.9 to −17.5)	−150.7 (−170.3 to −138.0)	7.8 (1.3 to 16.6)
pore ice HZ 6 core 5011-3 (n = 7)	−17.5 (−17.8 to −17.3)	−135.2 (−137.5 to −133.5)	5.0 (4.1 to 5.9)
pore ice HZ 5 core 5011-3 (n = 34)	−18.8 (−19.7 to −17.2)	−145.1 (−153.2 to −133.5)	5.1 (2.7 to 7.6)
pore ice HZ 4 core 5011-3 (n = 34)	−19.9 (−21.1 to −19.2)	−153.4 (−161.9 to −148.0)	6.0 (5.2 to 7.0)
pore ice HZ 3 core 5011-3 (n = 121)	−22.5 (−23.0 to −21.3)	−171.2 (−175.9 to −163.4)	7.8 (5.8 to 9.6)
pore ice HZ 2 core 5011-3 (n = 51)	−22.3 (−23.0 to −21.7)	−172.2 (−176.6 to −167.3)	6.5 (5.1 to 7.5)
pore ice HZ 1 core 5011-3 (n = 31)	−21.8 (−23.0 to −17.2)	−167.5 (−170.6 to −163.1)	6.7 (4.8 to 7.5)
pore ice (Holocene) (n = 31)	−19.1 (−19.9 to −18.4)	−146.6 (−151.5 to −140.4)	6.3 (3.3 to 7.7)
pore ice cores (Late Pleistocene) (n = 21)	−20.2 (−20.9 to −19.6)	−154.6 (−158.7 to −147.6)	7.3 (5.6 to 9.2)
ice wedge (Late Holocene) (n = 26)	−22.4 (−22.8 to −19.8)	−171.0 (−181.7 to −147.8)	9.2 (7.2 to 13.3)
ice wedge (Early Holocene) (n = 11)	−23.5 (−25.2 to −22.7)	−179.8 (−198.1 to −171.8)	8.5 (3.6 to 10.0)
lake ice (n = 4)	−18.5 (−18.0 to −19.4)	−146.3 (−149.9 to −140.5)	1.8 (−0.9 to 5.5)
rain (n = 17)	−14.6 (−25.9 to −6.2)	−121.9 (−202.8 to −72.9)	−4.8 (−23.1 to 5.9)
snow (n = 8)	−19.8 (−28.9 to −12.7)	−152.7 (−224.4 to −97.7)	6.3 (0.2 to 11.3)
streams*	−18.9 (−24.2 to −16.7)	−144.9 (−179.5 to 127.8)	6.7 (mean)
lake water column*	−19.8 (mean)	−154.9 (mean)	3.4 (mean)

* Data from: Wilkie et al. (2013).

CPD
9, 3993–4034, 2013

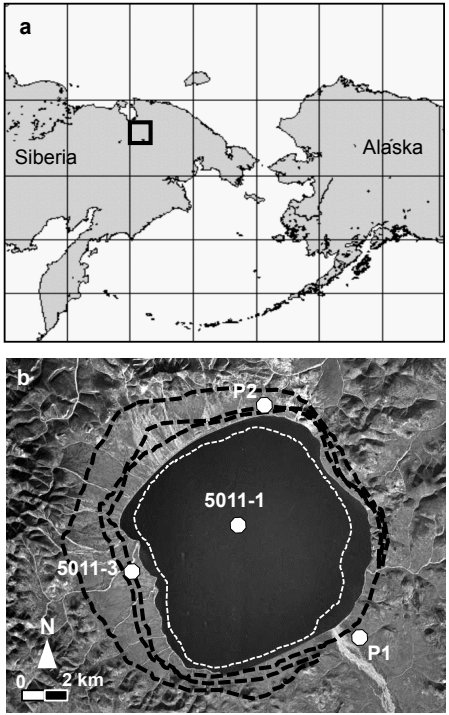

Fig. 1. (a) Geographic position of the El'gygytgyn Crater in NE Russia (black box). **(b)** A Corona image (source: USGS) showing Lake El'gygytgyn and drill sites 5011-3 on the permafrost flat west of the lake and 5011-1 in the lake. Dashed black lines indicate shorelines of the Middle Pleistocene (outer) and the Late Pleistocene (middle) according to Glushkova and Smirnov (2007), and the Allerød (inner) based on Schwamborn et al. (2008). The inner broken white line indicates the shoreline of the LGM according to Juschus et al. (2011). P1 and P2 denote the location of the short permafrost cores discussed in the text.

CPD
9, 3993–4034, 2013

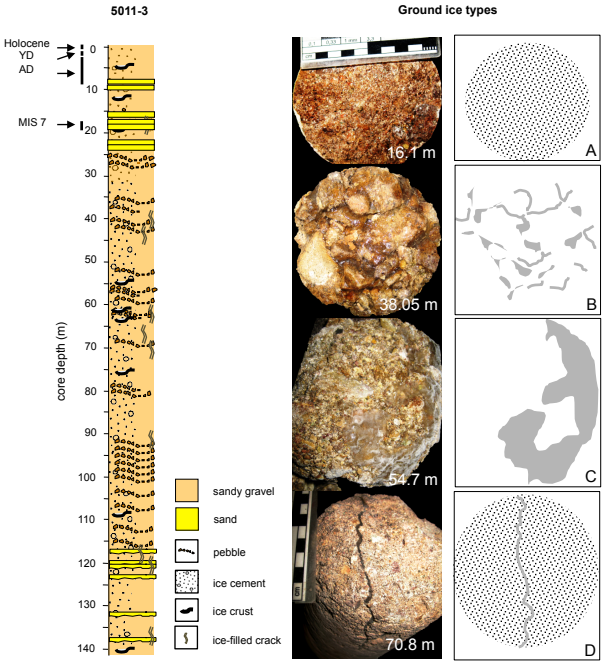

Fig. 2. Left: the lithological log of core 5011-3 including pollen-based stratigraphy from Andreev et al. (2012); YD = Younger Dryas, AD = Allerød, MIS = marine isotope stage. Right: photographic examples and generalized cryotexture of ground ice in the core. The scale is in cm, the core diameter is 11 cm. **(A)** Ice cement in a sandy matrix, **(B)** pore space fillings in a pebble layer, **(C)** ice crust around sandy gravel, **(D)** near-vertical ice vein in sandy gravel.

CPD
9, 3993–4034, 2013

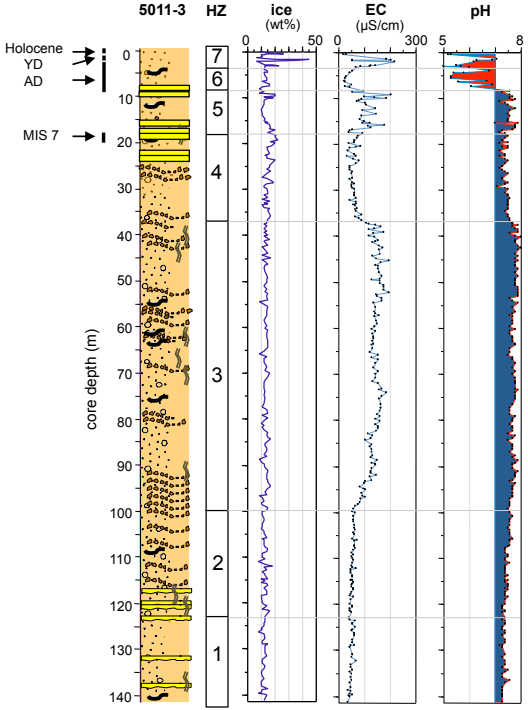

Fig. 3. The lithological log of core 5011-3 with ice content, EC (electrical conductivity), and pH of the ground ice. The subdivision into hydrological zones (HZs) is based on the EC record.

CPD
9, 3993–4034, 2013

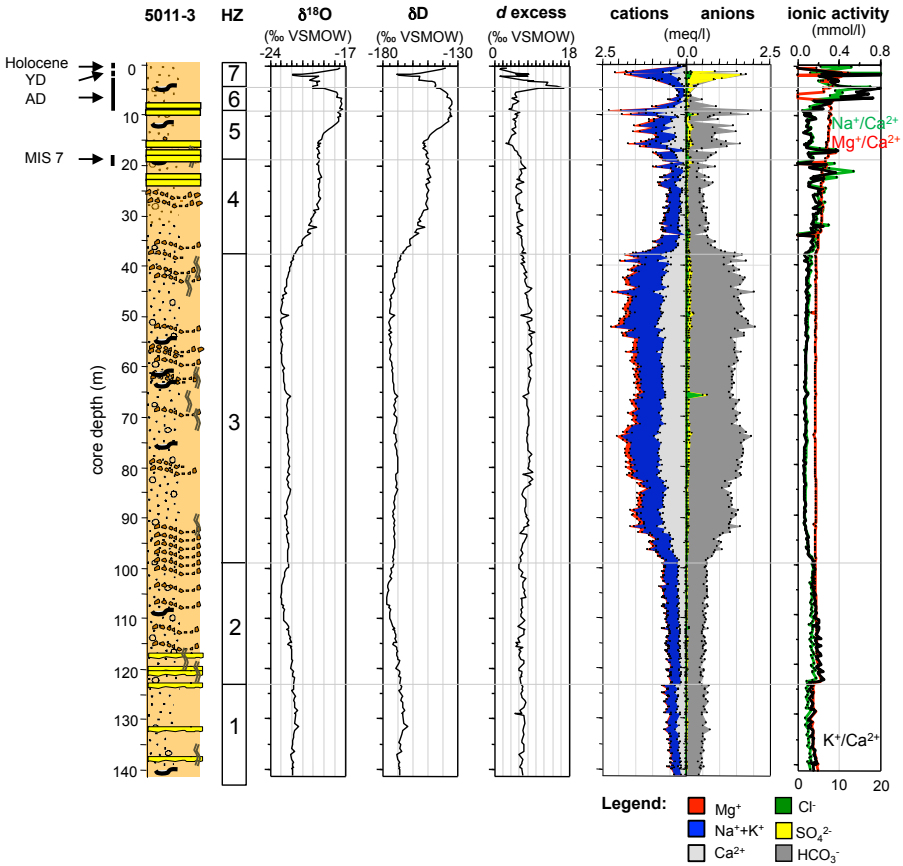

Fig. 4. The lithological log of core 5011-3 with stable isotope records ($\delta^{18}O$, δD, *d* excess), main cation and anion composition, and ion coefficients. Note: K^+ / Ca^{2+} lower scale; Na^+ / Ca^{2+} and Mg^+ / Ca^{2+} upper scale.

CPD
9, 3993–4034, 2013

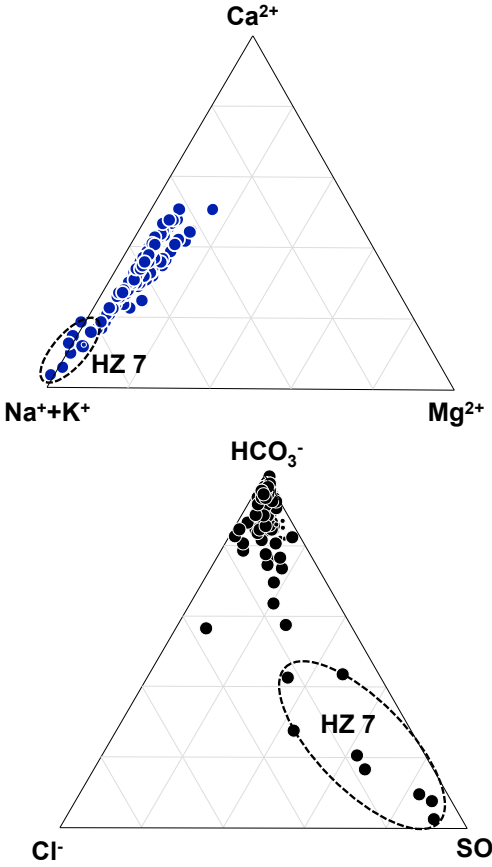

Fig. 5. Stable isotope composition of core 5011-3 pore ice, GMWL (Global Meteoric Water Line) after Craig (1961).

CPD
9, 3993–4034, 2013

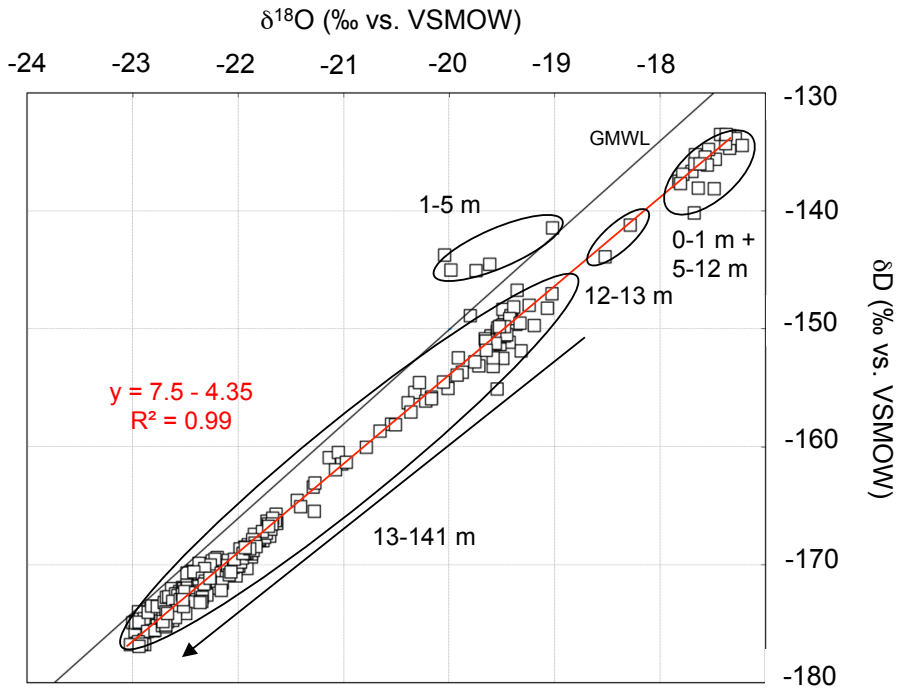

Fig. 6. Stable isotope composition of 5011-3 ground ice, which is subdivided into the seven hydrochemical zones (HZs) as discussed in the text. Other H_2O sample sets from the El'gygytgyn Crater are displayed for comparison with mean values and min. to max. ranges, GMWL (Global Meteoric Water Line) after Craig (1961), * data from Wilkie et al. (2012).

CPD
9, 3993–4034, 2013

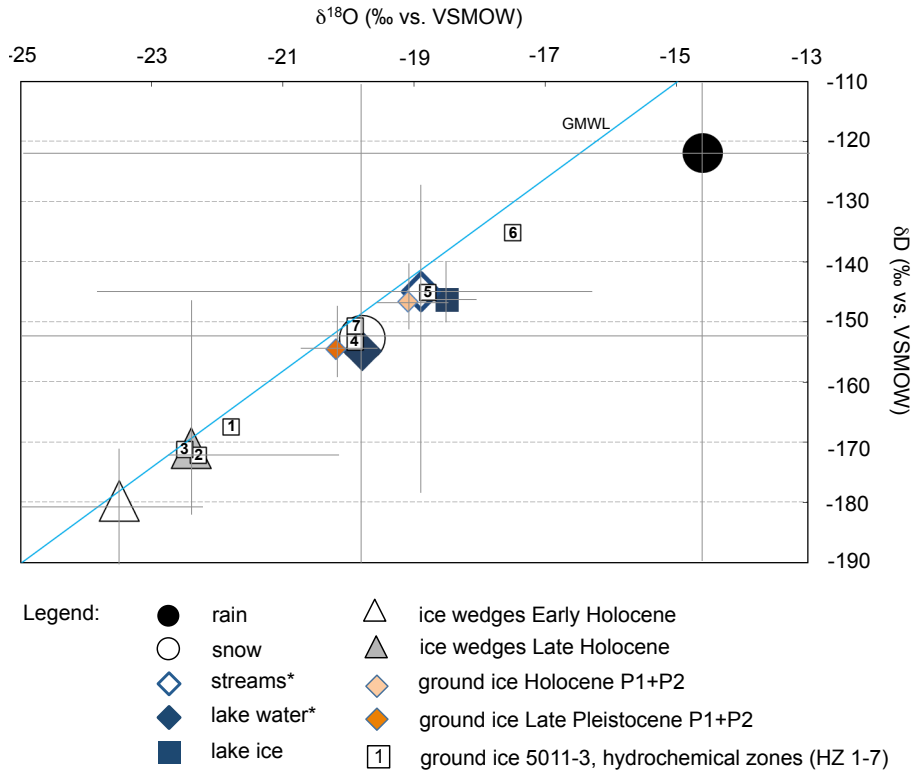

Fig. 7. Ternary diagram showing major cation (top) and anion (bottom) composition of core 5011-3 ground ice.

CPD
9, 3993–4034, 2013

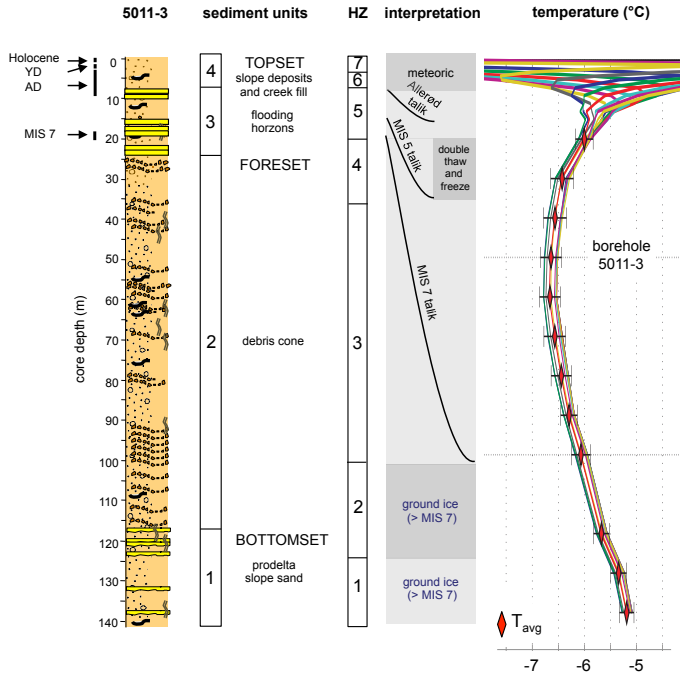

Fig. 8. Sediment record, sediment interpretation, hydrochemical interpretation, and temperature profile of the 5011-3 permafrost borehole. Sediment units are from Schwamborn et al. (2012), temperature profile with readings from 2010 is from Mottaghy et al. (2013); red diamonds = average temperature values.

CPD
9, 3993–4034, 2013

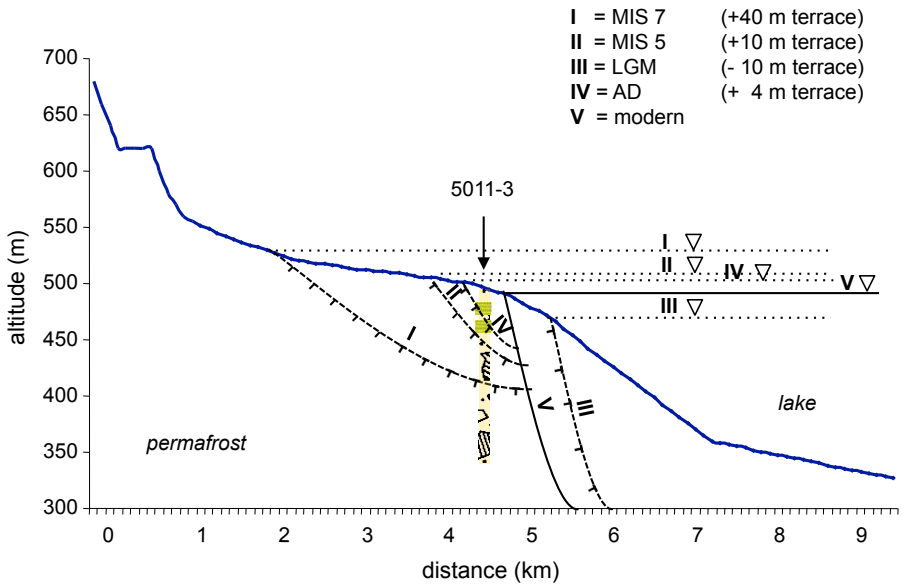

Fig. 9. Interpretation of talik migration and associated repeated thaw and refreeze in the course of Quaternary lake level fluctuations at the western edge of Lake El'gygytgyn.

CPD
9, 3993–4034, 2013